A Dipeptidyl Aminopeptidase–like Protein Remodels Gating Charge Dynamics in Kv4.2 Channels

Kevin Dougherty and Manuel Covarrubias

Department of Pathology, Anatomy and Cell Biology, Jefferson Medical College of Thomas Jefferson University, Philadelphia, PA 19107

Dipeptidyl aminopeptidase–like proteins (DPLPs) interact with Kv4 channels and thereby induce a profound remodeling of activation and inactivation gating. DPLPs are constitutive components of the neuronal Kv4 channel complex, and recent observations have suggested the critical functional role of the single transmembrane segment of these proteins (Zagha, E., A. Ozaita, S.Y. Chang, M.S. Nadal, U. Lin, M.J. Saganich, T. McCormack, K.O. Akinsanya, S.Y. Qi, and B. Rudy. 2005. *J. Biol. Chem.* 280:18853–18861). However, the underlying mechanism of action is unknown. We hypothesized that a unique interaction between the Kv4.2 channel and a DPLP found in brain (DPPX-S) may remodel the channel's voltage-sensing domain. To test this hypothesis, we implemented a robust experimental system to measure Kv4.2 gating currents and study gating charge dynamics in the absence and presence of DPPX-S. The results demonstrated that coexpression of Kv4.2 and DPPX-S causes a −26 mV parallel shift in the gating charge-voltage (Q-V) relationship. This shift is associated with faster outward movements of the gating charge over a broad range of relevant membrane potentials and accelerated gating charge return upon repolarization. In sharp contrast, DPPX-S had no effect on gating charge movements of the Shaker B Kv channel. We propose that DPPX-S destabilizes resting and intermediate states in the voltage-dependent activation pathway, which promotes the outward gating charge movement. The remodeling of gating charge dynamics may involve specific protein–protein interactions of the DPPX-S's transmembrane segment with the voltage-sensing and pore domains of the Kv4.2 channel. This mechanism may determine the characteristic fast operation of neuronal Kv4 channels in the subthreshold range of membrane potentials.

The Journal of General Physiology

INTRODUCTION

Auxiliary β subunits of Kv channels influence gating through diverse mechanisms, which in the best known instances involve direct interactions with intracellular domains of the channel (Jerng et al., 2004a; Heinemann and Hoshi, 2006). Interactions with transmembrane core domains (pore domain [PD] and voltage-sensing domain [VSD]) are also plausible and may help to explain the promiscuous effects of certain Kv channel β subunits (e.g., MiRP) on Kv channel permeation and gating (Hanlon and Wallace, 2002; Jerng et al., 2004a; Cai et al., 2006). The dipeptidyl aminopeptidase–like proteins (DPLPs), a recently discovered family of β subunits of neuronal Kv4 channels, may also use the latter type of interactions to influence function. DPLPs are analogous to the CD26 surface antigen, but lack enzymatic activity, and consist of a variable intracellular N-terminal domain followed by a single membrane-spanning segment and a large extracellular C-terminal domain (Kin et al., 2001; Nadal et al., 2003; Strop et al., 2004). DPLPs shift the voltage-dependent properties of Kv4 channels and accelerate their inactivation gating kinetics (Nadal et al., 2003; Jerng et al., 2004b; Ren et al., 2005; Zagha et al., 2005). Relative to the Kv4 α subunits expressed alone, Kv4–DPLP complexes exhibit a substantially leftward-shifted conductance-voltage relationship, which may result from remodeling different aspects of activation and inactivation gating (Ayer and Sigworth, 1997; Yifrach and MacKinnon, 2002). More concretely, however, a possible explanation for the leftward-shifted voltage dependence emerged from recent studies that identified putative interactions between the sole transmembrane segment of the DPLPs and discrete components of the Kv4 VSD (Ren et al., 2005; Zagha et al., 2005). Therefore, we hypothesized that the DPLP transmembrane segment may remodel the gating charge displacements that control Kv4 channel activation gating through interactions with the S4 voltage sensor. Such interactions may reshape the energetic landscape of the channel's voltage sensor during gating.

To test the hypothesis and gain more direct insights into the mechanisms of DPLP action, it is necessary to measure the Kv4 gating current (I_g). Under voltage-clamp conditions and in the absence of ion conduction, the gating charge displacements in the Kv channel

Correspondence to Manuel Covarrubias: Manuel.Covarrubias@jefferson.edu

The online version of this article contains supplemental material.

Abbreviations used in this paper: CTX, charybdotoxin; DPLP, dipeptidyl aminopeptidase–like protein; I_g, gating current; PD, pore domain; VSD, voltage-sensing domain; ZHA, Zagotta-Hoshi-Aldrich.

protein generate the nonlinear ON and OFF capacitive transients of the I_g, which correspond to the apparent outward and inward movements of the VSDs, respectively (Bezanilla, 2000, 2005). To block ion conduction and thereby unveil the Kv4.2 I_g for the first time, we engineered a charybdotoxin (CTX) binding site in the Kv4.2 PD (Kim et al., 2004). Then, to examine the remodeling of the I_g, the CTX-sensitive Kv4.2 channel was expressed heterologously in the absence and presence of DPPX-S, a DPLP expressed in the brain (Nadal et al., 2003). In a specific manner, DPPX-S induced dramatic changes in the voltage dependence and kinetics of the I_g, which result from promoting the movement of the Kv4.2 voltage sensor. These observations strongly suggest the presence of unique functional interactions between DPPX-S and the Kv4.2 VSD. To the best of our knowledge, no other Kv channel subfamily exhibits this type of functional remodeling by a specific auxiliary β subunit.

MATERIALS AND METHODS

Molecular Biology and Reagents

Kv4.2 cDNA (a gift from M. Sheng, Massachusetts Institute of Technology, Cambridge, MA) is maintained in pRc-cytomegalovirus (CMV; Invitrogen), whereas the DPPX-S cDNA (a gift from B. Rudy, New York University School of Medicine, New York, NY) is maintained in pSG5 (Stratagene). Shaker B Kv channels bearing the mutations W434F and T449V (a gift from R. Horn, Thomas Jefferson University, Philadelphia, PA) is maintained in the GWI-CMV vector (British Biotechnology). The $Kv4.2_{CTX}$ mutant was created with a site-directed mutagenesis kit (QuickChange; Stratagene) and confirmed by automated sequencing at the Nucleic Acid Facility of the Kimmel Cancer Center (Thomas Jefferson University, Philadelphia, PA). The transfection of tsA201 cells (a gift from R. Horn) was accomplished by the calcium-phosphate method (O'Leary and Horn, 1994), and a plasmid containing the CD8 gene was cotransfected to allow the identification of individual transfected cells by labeling them with beads bearing anti-CD8 antibody (Dynal). Recombinant CTX (98% pure) was purchased from Sigma-Aldrich.

Electrophysiology

Ionic currents were measured in the tight-seal whole-cell configuration of the patch-clamp method with the following pipette (intracellular) solution: 120 mM KF, 1 mM $CaCl_2$, 2 mM $MgCl_2$, 11 mM EGTA, and 10 mM HEPES, pH 7.2, adjusted with KOH; and the following external bath solution: 150 mM NaCl, 2 mM KCl, 1.5 mM $CaCl_2$, 1 mM $MgCl_2$, and 10 mM HEPES, pH 7.4, adjusted with NaOH. Series resistances (2–5 MΩ) were compensated to yield a total voltage error of ≤3 mV. Peak chord conductance (Gp) and its voltage dependence were calculated and analyzed as reported previously (Beck et al., 2002). I_g was measured with the following pipette (intracellular) solution: 105 mM CsF, 35 mM NaCl, 10 mM EGTA, and 10 mM HEPES, pH 7.4, adjusted with CsOH; and the following external solution: 135 mM NMG-Cl, 10 mM HEPES, 1 mM $MgCl_2$, and 1 mM $CaCl_2$, pH 7.4, adjusted with HCl. The I_g from Shaker Kv channels (W434F) was recorded with the Cs-containing pipette solution and the Na-containing bath solution described. A P/4 leak subtraction protocol consisting of four subpulses from a subsweep holding potential of −153 mV was used to subtract passive components of the total current and isolate the I_g. All I_g measurements were filtered at 5 kHz and sampled at 25 kHz. Analyses and graphical displays were produced with pClamp (version 9.0; Axon Instruments, Inc.) and Origin (version 7.0; OriginLab) software. The calculated liquid junction potential was subtracted off-line. All measurements were taken at room temperature (22–25°C).

To examine the effect of CTX on Kv4.2 wild type and $Kv4.2_{CTX}$, the corresponding mRNAs were injected into *Xenopus* oocytes alone or together with mRNA encoding DPPX-S. Using the two-electrode voltage-clamp technique reported previously (Beck et al., 2002), the Kv4.2 whole-oocyte currents were elicited by 400-ms voltage steps from −100 mV to +50 mV. A standard frog Ringer's saline in the bath was supplemented with 100 μg/ml BSA to avoid nonspecific binding of CTX to the recording chamber. CTX solutions were perfused manually by means of a disposable syringe, and immediately after each experiment, the recording chamber was bathed for at least 10 min in a concentrated 0.5 M NaCl solution to remove all residual CTX (Anderson et al., 1988).

Data Analysis and Model Simulations

Q_{ON} and Q_{OFF} values were obtained by integrating the area under the current trace for the length of the entire depolarization. Normalized Q-V relationships were described by assuming a Boltzmann function:

$$Q(V) = 1/(1 + \exp((V - V_{1/2})/k)),$$

and the Gp-V relationships were described by assuming a Boltzmann function raised to the fourth power; k represents the slope factor, and $V_{1/2}$ represents the midpoint voltage of the relationships. I_g relaxations were described by assuming an exponential function or the sum of exponential terms:

$$I_g(t) = \Sigma A_i \exp(-t/\tau_i),$$

where τ_i represents the time constant, and A_i represents the corresponding amplitude. The voltage-dependence of the time constants was determined according to the following equation:

$$\tau(V) = \tau_0 \exp(-ze_0V/k_BT),$$

where τ_0 represents the time constant at 0 mV, z represents the apparent charge, e_0 represents the electronic charge, and k_BT has its usual thermodynamic meaning. All data are expressed as mean ± SE, and the one-way ANOVA test was used to evaluate differences. Model simulations were conducted in the IChSim simulator developed by J. De Santiago-Castillo (www.ichsim.ionchannels.org). Rate constants were assumed to depend exponentially on membrane potential, and for comparative purposes, all simulated data were analyzed as described for the experimental observations.

Online Supplemental Material

Fig. S1 reports the results of an experiment that investigated the possible impact of DPPX-S on Shaker B gating charge dynamics. Online supplemental material is available at http://www.jgp.org/cgi/content/full/jgp.200609668/DC1.

RESULTS

DPPX-S Remodels Gating of the CTX-sensitive Kv4.2 Channel

Generally, the I_g is several orders of magnitude smaller than the corresponding ionic current. Thus, to examine

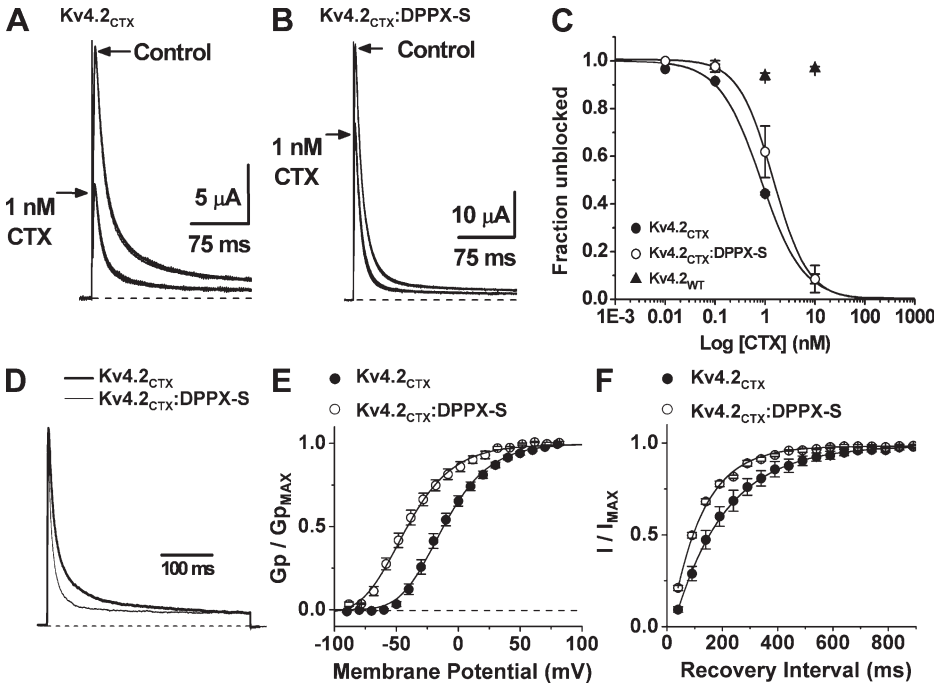

Figure 1. CTX sensitivity of Kv4.2 wild-type and $Kv4.2_{CTX}$ channels expressed in *Xenopus* oocytes. (A and B) Outward whole-oocyte K^+ currents mediated by $Kv4.2_{CTX}$ and $Kv4.2_{CTX}$:DPPX-S channels before (control saline in the bath) and after exposure to 1 nM CTX in control saline (see Materials and methods). Currents were elicited by 400-ms step depolarizations from −100 mV to +50 mV. (C) Dose–response relationships for $Kv4.2_{WT}$, $Kv4.2_{CTX}$, and $Kv4.2_{CTX}$:DPPX-S channels. Both $Kv4.2_{CTX}$ and $Kv4.2_{CTX}$:DPPX-S channels are sensitive to CTX in the subnanomolar or nanomolar range. The solid line superimposed on the symbols is the best-fit Hill equation of this form: $y = (A2 + (A1 - A2))/(1 + (x/K_d)^h)$. $A1$ and $A2$ represent the maximum and minimum, K_d represents the apparent disassociation constant, and h represents the Hill coefficient. The best-fit parameters were as follows: $Kv4.2_{CTX}$, K_d = 0.83 nM and h = 1.04; and $Kv4.2_{CTX}$:DPPX-S, K_d = 1.48 nM and h = 1.27 ($n \geq 3$ experiments). DPPX-S does not significantly alter the CTX sensitivity of $Kv.2_{CTX}$ channels ($P > 0.05$ by one-way ANOVA). Data are expressed as mean ± SE. (D) Whole-cell (tsA201; see Materials and methods) $Kv4.2_{CTX}$ currents evoked by a 400-ms step depolarization to +32 mV from a holding potential of −108 mV. Note that the macroscopic inactivation of $Kv4.2_{CTX}$ channels is accelerated by DPPX-S. (E) Gp-V relationships of $Kv4.2_{CTX}$ channels expressed alone or coexpressed with DPPX-S. The solid lines are best-fit fourth-order Boltzmann functions with the following parameters: $V_{1/2}$ ($Kv4.2_{CTX}$) = −13.2 mV, k ($Kv4.2_{CTX}$) = 23.2 mV; and $V_{1/2}$ ($Kv4.2_{CTX}$:DPPX-S) = −43.6 mV, k ($Kv4.2_{CTX}$:DPPX) = 23.6 mV. The dashed line indicates the zero-conductance level. (F) Recovery from inactivation at −110 mV. The solid lines are the best-fit exponential functions with the following parameters: τ ($Kv4.2_{CTX}$) = 186 ms; and τ ($Kv4.2_{CTX}$:DPPX-S) = 116 ms. The changes induced by DPPX-S are similar to those reported by others for Kv4.2 wild type (Nadal et al., 2003; Jerng et al., 2004b). Data in E and F are expressed as mean ± SE.

the effects of DPPX-S on Kv4.2 gating charge dynamics, the ionic current must be eliminated. Kv4 channels are typically insensitive to external blockers of most Kv channels (i.e., TEA and pore toxins). Therefore, according to a previous study (Kim et al., 2004), we engineered a Kv4.2 mutant with three pore substitutions (K353G, A359D, and K379V) that are sufficient to confer high sensitivity to CTX, a potent K^+ channel pore toxin (Fig. 1, A–C). The voltage-dependent and kinetic properties of the ionic currents mediated by the Kv4.2 wild type and the Kv4.2 triple mutant ($Kv4.2_{CTX}$) were generally similar, as shown previously (Fig. 1, D–F; and Table I; Kim et al., 2004). An exception was the peak conductance-voltage relationship (Gp-V relationship) of the $Kv4.2_{CTX}$ channel, which appeared moderately shifted to the left (Table I). This shift was not investigated further. More importantly, however, DPPX-S remodeled the Kv4.2 wild-type and $Kv4.2_{CTX}$ ionic currents similarly and as reported by others (Nadal et al., 2003; Jerng et al., 2004b, 2005; Zagha et al., 2005). The hallmark changes include faster macroscopic inactivation at depolarized membrane potentials, a leftward-shifted Gp-V relationship, and faster recovery from inactivation at hyperpolarized membrane potentials (Fig. 1, D–F; and Table I). These results justified the use of the $Kv4.2_{CTX}$ channel to investigate the remodeling of gating charge dynamics by DPPX-S.

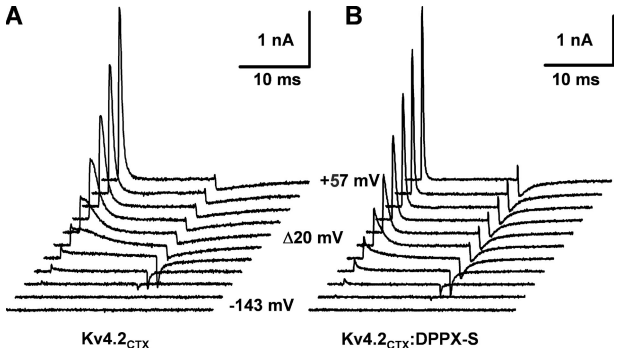

Figure 2. I_g from $Kv4.2_{CTX}$ and $Kv4.2_{CTX}$:DPPX-S channels. (A) I_g from $Kv4.2_{CTX}$ channels expressed in tsA201 cells in the presence of 100 nM CTX and 105 mM intracellular CsF. From a holding potential of −153 mV, currents were elicited by a series of 12-ms voltage steps between −143 and +57 mV in 20-mV increments. (B) I_g from $Kv4.2_{CTX}$:DPPX-S channels recorded under conditions identical to those used in A. Note the acceleration of the I_g-ON and I_g-OFF kinetics in the presence of DPPX-S.

TABLE I

Activation Parameters of Kv4.2 and Shaker B channels

	Gp-V	Gp-V	Q_{ON}-V	Q_{ON}-V	Q_{ON} vs. Q_{OFF}
	$V_{1/2}$ (mV)	k (mV)	$V_{1/2}$ (mV)	Effective charge e_0	Slope
$Kv4.2_{WT}$	−6.58 ± 1.5[a] (4)	26.7 ± 1.1 (4)			
$Kv4.2_{WT}$:DPPX	−26.9 ± 2[a] (3)	22.2 ± 1.6 (3)			
$Kv4.2_{CTX}$	−14 ± 1.8[b,c] (11)	23 ± 0.8 (11)	−46.9 ± 1.7[d] (6)	3.33 ± 0.2 (6)	0.97 ± 0.02 (4)
$Kv4.2_{CTX}$:DPPX	−41.9 ± 3.2[b,c] (5)	23.4 ± 1.5 (5)	−73.2 ± 0.9[d] (7)	3.1 ± 0.1 (7)	1.02 ± 0.03 (4)
Shaker B W434F			−46.3 ± 2.3[e] (4)	2.77 ± 0.2 (4)	
Shaker B W434F + DPPX-S			−52.2 ± 0.4[e] (4)	3.1 ± 0.2 (4)	

[a]The leftward shift induced by DPPX-S ($\Delta V_{1/2}$ = −20 mV) is highly significant at $P < 0.01$.

[b]The leftward shift induced by DPPX-S ($\Delta V_{1/2}$ = −28 mV) is highly significant at $P < 0.01$.

[c]The Gp-V midpoint voltages (at $Gp/Gp_{max} = 0.5$) of the $Kv4.2_{CTX}$ mutant in the absence and presence of DPPX-S were considerably different from those of the $Kv4.2_{WT}$. This difference was not examined further.

[d]The leftward shift induced by DPPX-S ($\Delta V_{1/2}$ = −26 mV) is highly significant at $P < 0.0001$.

[e]The leftward shift induced by DPPX-S ($\Delta V_{1/2}$ = −6 mV) appeared modestly significant at $P = 0.045$. Differences between other parameters (k and effective charge Z) were not statistically significant for all pairs in the absence and presence of DPPX-S. The number of independent determinations for all tabulated measurements is indicated in parentheses.

$Kv4.2_{CTX}$ I_g and Gating Charge Dynamics in the Absence and Presence of DPPX-S

A previous study demonstrated that CTX effectively blocks Shaker Kv1 channels but has no effect on the I_g (Schoppa and Sigworth, 1998). Thus, to isolate the $Kv4.2_{CTX}$ I_g, the cells were exposed to saturating concentrations of CTX (∼100 nM), which completely eliminates the $Kv4.2_{CTX}$ ionic current (Fig. 1 C). Under these conditions and in response to step depolarizations, the ON and OFF components of the I_g were observed clearly (Fig. 2, A and B). The peak amplitude of the I_g-ON was typically >1 nA at the more depolarized membrane potentials. Qualitatively, the $Kv4.2_{CTX}$ I_g exhibits voltage dependence and kinetics that are characteristic of Kv channels (Bezanilla, 2000). The gating charge increases sharply with depolarization (Fig. 2 and Fig. 3, A and B), and consistent with the capacitive nature of the I_g, the ON and OFF gating charge–voltage relations (Q_{ON}-V and Q_{OFF}-V relations, respectively) are equal (i.e., the gating charge is conserved; Fig. 3, C and D). Also, the overall kinetics of the I_g-ON became faster with membrane depolarization (see next paragraph; Fig. 2). The effects of DPPX-S on the I_g were striking. Coexpression of $Kv4.2_{CTX}$ and DPPX-S resulted in faster I_g-ON and I_g-OFF (Fig. 2, A and B) and a parallel leftward shift of the Q_{ON}-V relationship (Fig. 4 and Table I). The magnitude of this shift (−26 mV) is comparable to that of the Gp-V relationship, as described in the previous section (Fig. 1 E and Table I).

To characterize the kinetic effects of DPPX-S more quantitatively, the relaxation of the I_g-ON was approximated as an exponential decay (Fig. 5 A). In the absence and presence of DPPX-S, this analysis provided an overall evaluation of the forward steps in the voltage-dependent activation process. In both conditions, the best-fit exponentials yielded voltage-dependent time constants that decrease with membrane depolarization. Clearly, however, DPPX-S reduced these time constants uniformly at membrane potentials greater than or equal to −50 mV (Fig. 5 B). The time constant–voltage relationships were described by assuming exponential voltage dependencies in the absence and presence of DPPX-S (Fig. 5 B). At 0 mV, the time constant (τ_0) is fivefold faster in the presence of DPPX-S than in its absence, but the effective valence (z) was not affected by DPPX-S (∼1 e_0). The I_g-OFF relaxations at −153 mV were better described by assuming the sum of two exponential terms (Fig. 5, C and D). The fractional amplitudes of the exponential terms are not affected much by DPPX-S (Fig. 5 D). In contrast, DPPX-S decreases both the fast and slow I_g-OFF time constants by 3- and 3.7-fold, respectively (Fig. 5 D). Overall, the analysis of the $Kv4.2_{CTX}$ I_g demonstrates a general acceleration of gating charge dynamics by DPPX-S.

DPPX-S Promotes Voltage-dependent Activation of Kv4.2 Channels

The effects of DPPX-S on Kv4.2 gating charge dynamics could result from selective changes in the voltage-dependent transitions of the activation pathway. To test this hypothesis qualitatively, we simulated the I_g by assuming a general form of the Zagotta-Hoshi-Aldrich (ZHA) kinetic model without the final C_F state (Zagotta et al., 1994). Currently, there is no specific kinetic model that explains all major features of Kv4.2 channel gating unambiguously. In the ZHA model, each subunit of the Kv channel tetramer acts independently and undergoes two sequential voltage-dependent transitions that correspond to the major movements of the voltage sensor. Assuming that DPPX-S induces a fivefold increase in the forward rates constants of both transitions ($\alpha \times 5$ and $\gamma \times 5$) was sufficient to simulate the main

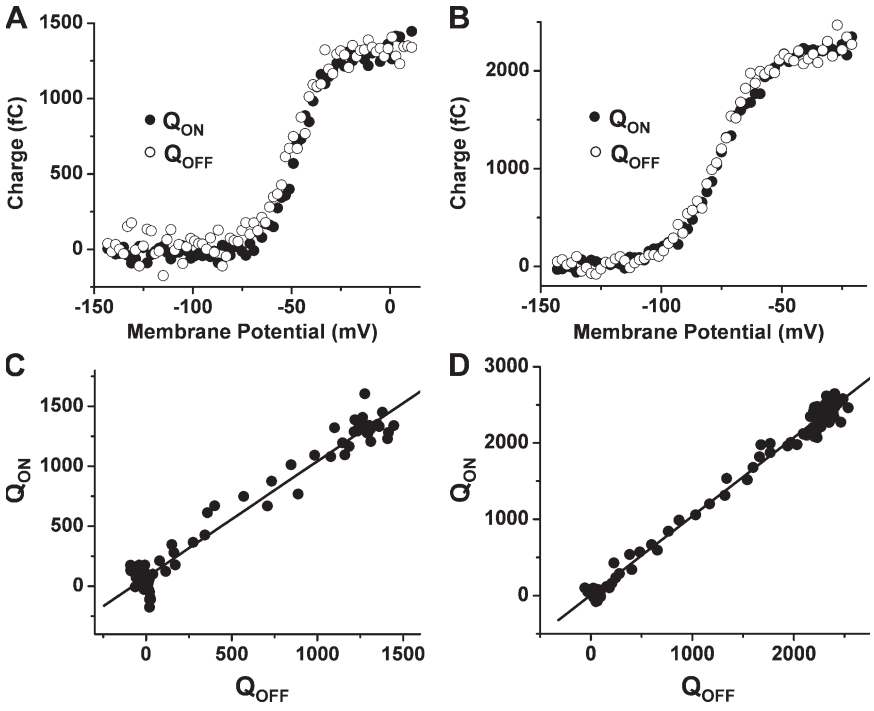

Figure 3. Charge conservation in Kv4.2$_{CTX}$ and Kv4.2$_{CTX}$:DPPX-S channels. (A) Q_{ON}-V and Q_{OFF}-V relationships from Kv4.2$_{CTX}$ channels. (B) Q_{ON}-V and Q_{OFF}-V relationships from Kv4.2$_{CTX}$:DPPX-S channels. (C) Q_{ON} and Q_{OFF} values from Kv4.2$_{CTX}$ channels are strongly correlated with a slope of 0.97 (r = 0.98). (D) Q_{ON} and Q_{OFF} values from Kv4.2$_{CTX}$:DPPX-S channels are strongly correlated with a slope of 1.03 (r = 0.99).

observed changes closely (Fig. 6), which are (a) dramatically accelerated I_g-ON; (b) uniformly reduced time constants of the I_g-ON relaxation over the examined range of membrane potentials (approximately fivefold smaller at 0 mV); (c) a leftward-shifted Q_{ON}-V relationship; and (d) a leftward-shifted G-V relationship. As observed, both relationships were shifted by −25 mV. Although there is a good general agreement between the simulated and observed data, a limitation of the simulations is that the ZHA model does not include coupled inactivation transitions. As a result, the simulated steady-state activation curves (Fig. 6 D) differed from the observed data (Fig. 1 E), because the Gp-V relationship is influenced by inactivation and late opening transitions (Ayer and Sigworth, 1997; Yifrach and MacKinnon, 2002), which are not fully characterized in Kv4 channels.

The I_g from the Shaker B Kv Channel Is Not Affected by DPPX-S

DPPX-S is a membrane protein with a single transmembrane segment that could interact promiscuously with the VSD in the transmembrane core of other Kv channels and thereby alter their biophysical properties. To test this possibility, we investigated the effect of DPPX-S on the I_g of the Shaker B channel. The I_g from nonconducting Shaker B channels (W434F mutant) and Shaker B channels exposed to CTX or in the absence of permeant ions exhibits similar properties (Perozo et al., 1993; Schoppa and Sigworth, 1998). Therefore, we expressed the Shaker B W434F mutant alone or coexpressed it with DPPX-S in tsA201 cells and studied the I_g. This I_g is typically >1 nA at positive membrane potentials and exhibits the characteristic biophysical properties that fully agree with previous studies (Fig. S1, available at http://www.jgp.org/cgi/content/full/jgp.200609668/DC1). In sharp contrast with the results obtained with the Kv4.2$_{CTX}$ channel, however, DPPX-S had no significant effects on the kinetics of the I_g or the voltage dependence of the gating charge (Fig. S1 and Table I). At the

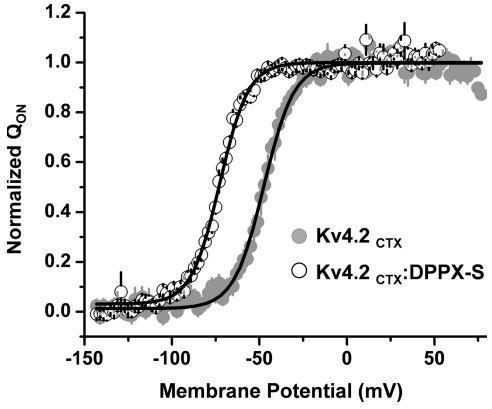

Figure 4. Normalized Q_{ON}-V relationships from Kv4.2$_{CTX}$ and Kv4.2$_{CTX}$:DPPX-S channels. The Q_{ON}-V relationships were described by assuming a Boltzmann function (see Materials and methods) with the following best-fit parameters (Table I): $V_{1/2}$ (Kv4.2 $_{CTX}$) = −47 mV and z (Kv4.2 $_{CTX}$) = 2.98 e_0 (n = 6); and $V_{1/2}$ (Kv4.2$_{CTX}$:DPPX-S) = −73 mV and z (Kv4.2$_{CTX}$:DPPX-S) = 3.04 e_0 (n = 7). Current traces were sampled in 2-mV increments. The mean Q_{max} values in the absence and presence of DPPX-S were 107 ± 28 fC/pF (n = 6) and 98 ± 21 fC/pF (n = 7), respectively. Data are expressed as mean ± SE.

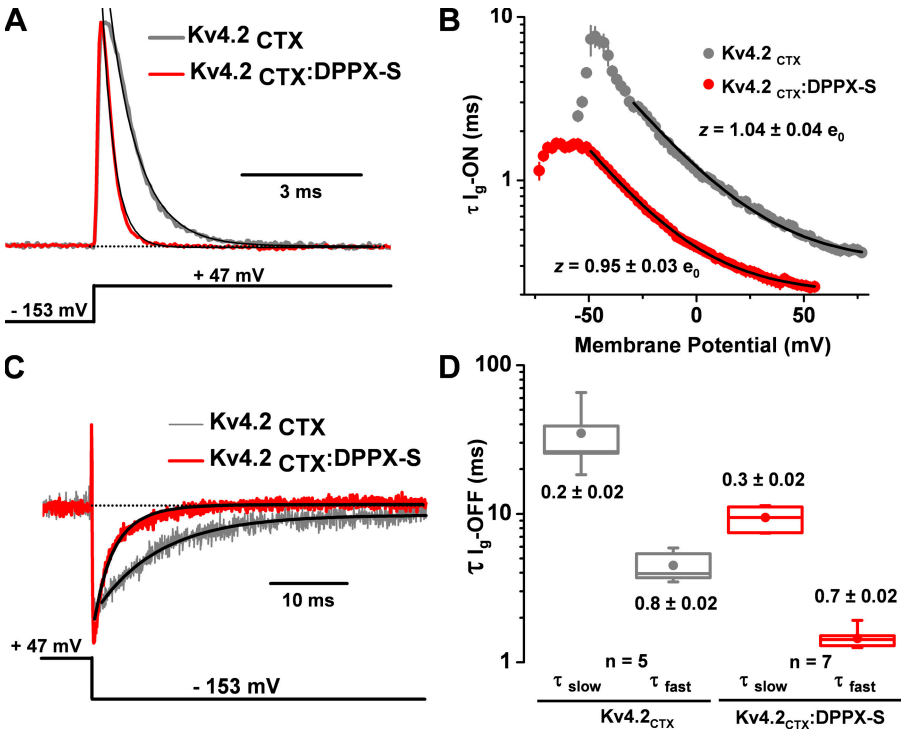

Figure 5. $Kv4.2_{CTX}$ I_g kinetics in the absence and presence of DPPX-S. (A) I_g elicited by a voltage step to +47 mV from a holding potential of −153 mV for both $Kv4.2_{CTX}$ (gray traces) and $Kv4.2_{CTX}$:DPPX-S (red traces) channels. Note the accelerated decay of the $Kv4.2_{CTX}$:DPPX-S I_g. Continuous black lines represent the best-fit exponential decays. The dotted line is the zero-current level. (B) Time constants resulting from the exponential fits plotted against membrane potential. The continuous black lines represent the best-fit exponential (see Materials and methods). Near the midpoint voltage of the Q_{ON}-V relationships (data points excluded from the exponential fit), the I_g relaxations were described by assuming the sum of two exponential terms; thus, the corresponding data points are the weighted means of the time constants. Note that at all voltages, the $Kv4.2_{CTX}$:DPPX-S I_g-ON exhibits faster time constants than its $Kv4.2_{CTX}$ counterparts. The effective valences derived from this analysis were 1.04 ± 0.04 e_0 for $Kv4.2_{CTX}$ (n = 6) and 0.95 ± 0.03 e_0 for $Kv4.2_{CTX}$:DPPX-S (n = 7). (C) OFF I_g from both $Kv4.2_{CTX}$ (gray traces) and $Kv4.2_{CTX}$:DPPX-S (red traces) channels resulting from a repolarizing voltage step from +47 mV to −153 mV. Continuous black lines represent the best-fit sum of two exponential terms. (D) Box plot of the I_g-OFF time constants (repolarizations to −153 mV from +47 mV). The borders of the boxes represent the 25th and 75th percentiles, whereas the median and mean are represented by a closed circle and a horizontal line in the box, respectively. Error bars represent the 5th and 95th percentiles, respectively. The fractional amplitudes of the exponential terms are indicated by the numbers displayed below or above the corresponding boxes.

protein level, this result is consistent with the absence of a physical interaction between Kv1.4, a Shaker-type channel, and DPPY (Ren et al., 2005), but it does not support another recent study, which reported effects of DPPY on Kv1.4 ionic current kinetics (Li et al., 2006). Thus, the dramatic remodeling of $Kv4.2_{CTX}$ gating charge dynamics by DPPX-S is relatively specific.

DISCUSSION

In vivo, most Kv channels exist as part of macromolecular complexes that include a variety of specific β subunits (Hanlon and Wallace, 2002). Although there is considerable information on the mechanisms responsible for the biophysical effects of β subunits that interact with intracellular channel domains (T1 or the C-terminal region; Jerng et al., 2004a; Callsen et al., 2005; Heinemann and Hoshi, 2006), much less is known about those that may interact with the transmembrane domains of the channel's core (PD and VSD; Hanlon and Wallace, 2002; Jerng et al., 2004a; Cai et al., 2006). The Kv channel VSD has been the subject of intense research and controversy, and major breakthroughs have been made toward solving the mechanisms of voltage-dependent activation (Ahern and Horn, 2004, 2005; Chanda et al., 2005; Long et al., 2005b; Posson et al., 2005; Tombola et al., 2006). Nevertheless, the possible remodeling of the Kv channel VSD by specific membrane-spanning β subunits that affect voltage-dependent gating remained largely unexplored. Therefore, we investigated the interactions between DPPX-S and Kv4.2 channels by examining gating charge dynamics. The main results led us to suggest that DPPX-S promotes the outward movement of the Kv4.2 gating charge in a specific manner.

The Impact of DPPX-S on Kv4.2 Gating Charge Dynamics: Mechanistic Implications

A recent study suggested that residues in the S1 and S2 transmembrane segments of Kv4.3 channels are critical determinants of DPLP action (Ren et al., 2005). In addition, this and other studies have suggested that the functional remodeling of Kv4 channels by DPLPs depends on transmembrane interactions involving the single membrane-spanning segment of DPLPs (Ren et al., 2005; Zagha et al., 2005). Thus, given the results of this study, it is tantalizing to propose that the transmembrane segment of DPPX-S is influencing the relative stability of various conformations of the VSD through changes in the membrane environment and packing of the channel's core. DPPX-S could thereby facilitate the shift of the VSD conformations from reluctant to permissive.

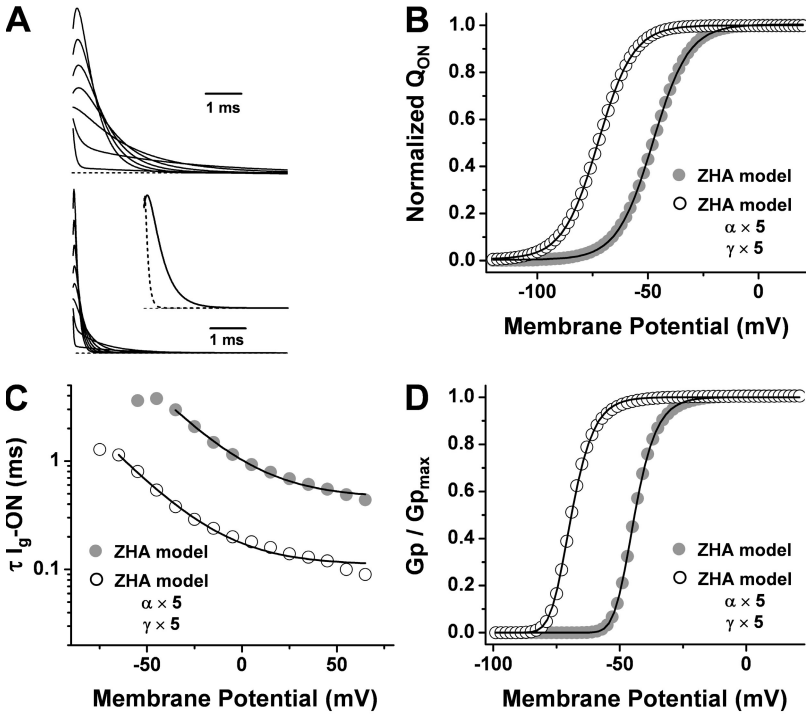

Figure 6. Kinetic modeling of voltage-dependent gating in the absence and presence of DPPX-S. All simulations assume the ZHA model of Kv channel gating and were conducted as described in Materials and methods. (A) Simulated I_g evoked by 6-ms step depolarizations (top, −55 to +65 mV; bottom, −75 to +65 mV; both in 20-mV increments) to the indicated membrane potentials and assuming a holding potential of −153 mV. The top and bottom families of traces simulate Kv4.2 I_g in the absence and presence of DPPX-S, respectively. The simulation parameters are those reported in Table I of Zagotta et al. (1994), except that for the bottom family of traces, the forward rate constants (α and δ) of the two sequential transitions in each subunit of the channel were increased fivefold. The inset compares control (continuous line) and accelerated (dashed line) I_g evoked by depolarizations to +45 mV. In all plots (B–D), the simulations that assume accelerated gating are depicted by open symbols. (B) Simulated Q_{ON}-V relationships. Q_{ON} was simulated in 2-mV increments. The continuous lines superimposed on the simulated data symbols are best-fit Boltzmann functions (see Materials and methods) with the following parameters: $V_{1/2}$ (closed symbols) = −48 mV and z (closed symbols) = 3.2 e_0; and $V_{1/2}$ (open symbols) = −73 mV and z (open symbols) = 3.2 e_0. The $\Delta V_{1/2}$ = −25 mV. (C) Simulated time constant–voltage relationships. The time constants were derived by approximating the simulated I_g relaxations with an exponential function (as done for the observed I_g; see Results). The initial fast phase at low voltages and the rising phase at high voltages were excluded from this analysis. The continuous lines superimposed on the simulated data symbols are best-fit exponential functions that describe the voltage dependence of the time constants (see Materials and methods). The effective valences derived from this analysis were 1.08 e_0 (closed symbols) and 1.09 (open symbols) e_0. (D) Simulated G-V relationships. The plots were generated from the steady-state level of the simulated ionic currents at the indicated membrane potentials (2-mV increments). The chord conductance (G) was calculated by assuming a reversal potential of −100 mV. The continuous lines superimposed on the simulated data symbols are the best-fit fourth-order Boltzmann functions with the following parameters: $V_{1/2}$ (closed symbols) = −45 mV and k (closed symbols) = 5.4 mV; and $V_{1/2}$ (open symbols) = −70 mV and k (open symbols) = 5.5 mV. $V_{1/2}$ is the calculated voltage at Gp/Gp_{max} = 0.5, and k is the slope factor. The $\Delta V_{1/2}$ = −25 mV.

Kinetic modeling (Fig. 6) showed that acceleration of the outward gating charge movement induced by DPPX-S may result from destabilization of the resting and intermediate states of the Kv4.2 subunits, which promotes the permissive conformation of the VSD. These results are consistent with reduced energy barriers of the voltage-dependent transitions in the presence of DPPX-S; therefore, this auxiliary subunit may exert a catalytic effect on voltage-dependent gating of Kv4.2 channels.

By promoting voltage-dependent activation, DPPX-S may also accelerate coupled inactivation indirectly, which could account in part for the observed acceleration of the development of inactivation (Fig. 1). The extent of additional direct effects of DPPX-S on Kv4 inactivation gating is not yet clear. The acceleration of the I_g-OFF by DPPX-S (Fig. 5, C and D) may involve interactions between inactivation and gating charge movement. A concrete possibility is that recovery from inactivation limits the observed rate of return or remobilization of the gating charge (Roux et al., 1998). Thus, given that DPPX-S accelerates the recovery from inactivation (Fig. 1 E), the return of the gating charge is consequently faster.

A physical interaction between DPPX-S and the Kv4.2 VSD is plausible in the light of the recently published crystal structure of a mammalian Kv channel (Long et al., 2005a). Four VSDs surround the pore structure in the center of the tetramer and are substantially exposed to possible interactions with neighboring membrane proteins. Those interactions may involve specific contacts between the transmembrane segment of DPPX-S, the VSD, and the PD. Further biochemical and structural studies are necessary to understand the stoichiometry and architecture of such a Kv channel complex, the identity of the unique interactions, and the physical basis of the functional remodeling. The presence of the DPPX-S transmembrane segments as part of the Kv4 channel complex may reconfigure the architecture of the VSD in an important way.

Neurophysiological Implications of Remodeling Kv4.2 Gating Charge Dynamics by DPPX-S

Various studies suggest strongly that DPLPs are integral parts of the native Kv4 channel complex that underlies the somatodendritic A-type K^+ current (I_{SA}) in the

mammalian brain (Nadal et al., 2003; Jerng et al., 2004a, 2005). Critical functions of I_{SA} include the regulation of repetitive firing frequency, dampening of backpropagating action potentials, and compartmentalization of dendritic excitability (Jerng et al., 2004a). These functional roles depend on the ability of I_{SA} to operate in the subthreshold range of membrane potentials. By remodeling gating charge dynamics, DPPX-S could be the key determining factor of I_{SA} operation in the subthreshold range of membrane potentials. KChIPs are also integral components of native Kv4 channels (Jerng et al., 2004a); however, these cytosolic proteins interact with the N-terminal region and the intracellular T1 domain directly (Zhou et al., 2004; Callsen et al., 2005) and are not likely to interact with the VSD or the PD. The extent to which KChIPs may remodel gating charge dynamics through indirect allosteric interactions has not been investigated.

Conclusion

This study reports the profound tune-up of the Kv4.2 VSD by a specific β subunit (DPPX-S). Based on these observations and current knowledge, this study strongly supports the concept of specific interactions between the single membrane-spanning segment of DPPX-S and the channel's VSD in the transmembrane core. The typical operating membrane potential range of the neuronal Kv4 channel may depend on this exceptional interaction.

We thank Drs. R. Horn and T. Hoshi for their critical reading of the manuscript and Dr. B. Rudy for providing DPPX-S cDNA, as well as critical comments. Also, we thank Drs. R. Horn and C. Ahern for helpful advice in the initial stages of this study; members of the Covarrubias lab for continuous feedback and support; and Dr. José De Santiago-Castillo for help with kinetic modeling and the use of IChSim (www.ichsim.ionchannels.org).

This work was supported by the National Institutes of Health (grants R01 NS032337 and T32 AA07463 to M. Covarrubias and K. Dougherty, respectively).

Olaf S. Anderson served as editor.

Submitted: 19 September 2006
Accepted: 6 November 2006

REFERENCES

Ahern, C.A., and R. Horn. 2004. Stirring up controversy with a voltage sensor paddle. *Trends Neurosci.* 27:303–307.

Ahern, C.A., and R. Horn. 2005. Focused electric field across the voltage sensor of potassium channels. *Neuron.* 48:25–29.

Anderson, C.S., R. MacKinnon, C. Smith, and C. Miller. 1988. Charybdotoxin Block of Single Ca^{2+}-activated K^+ Channels. Effects of Channel Gating, Voltage, and Ionic Strength. *J. Gen. Physiol.* 91:317–333.

Ayer, R.K.J., and F.J. Sigworth. 1997. Enhanced closed-state inactivation in a mutant Shaker K^+ channel. *J. Membr. Biol.* 157:215–230.

Beck, E.J., M. Bowlby, W.F. An, K.J. Rhodes, and M. Covarrubias. 2002. Remodeling inactivation gating of Kv4 channels by KChIP-1, a small-molecular-weight calcium binding protein. *J. Physiol.* 538:691–706.

Bezanilla, F. 2000. The voltage sensor in voltage-dependent ion channels. *Physiol. Rev.* 80:555–592.

Bezanilla, F. 2005. Voltage-gated ion channels. *IEEE Trans. Nanobioscience.* 4:34–48.

Cai, S.Q., K.H. Park, and F. Sesti. 2006. An evolutionarily conserved family of accessory subunits of K^+ channels. *Cell Biochem. Biophys.* 46:91–99.

Callsen, B., D. Isbrandt, K. Sauter, L.S. Hartmann, O. Pongs, and R. Bähring. 2005. Contribution of N- and C-terminal channel domains to Kv channel interacting proteins in a mammalian cell line. *J. Physiol.* 568:397–412.

Chanda, B., O.K. Asamoah, R. Blunck, B. Roux, and F. Bezanilla. 2005. Gating charge displacement in voltage-gated ion channels involves limited transmembrane movement. *Nature.* 436:852–856.

Hanlon, M.R., and B.A. Wallace. 2002. Structure and function of voltage-dependent ion channel regulatory beta subunits. *Biochemistry.* 41:2886–2894.

Heinemann, S.H., and T. Hoshi. 2006. Multifunctional potassium channels: electrical switches and redox enzymes, all in one. *Sci. STKE.* 2006:pe33.

Jerng, H.H., K. Kunjilwar, and P.J. Pfaffinger. 2005. Multiprotein assembly of Kv4.2, KChIP3 and DPP10 produces ternary channel complexes with I_{SA}-like properties. *J. Physiol.* 568:767–788.

Jerng, H.H., P.J. Pfaffinger, and M. Covarrubias. 2004a. Molecular physiology and modulation of somatodendritic A-type potassium channels. *Mol. Cell. Neurosci.* 27:343–369.

Jerng, H.H., Y. Qian, and P.J. Pfaffinger. 2004b. Modulation of Kv4.2 channel expression and gating by dipeptidyl peptidase 10 (DPP10). *Biophys. J.* 87:2380–2396.

Kim, L.A., J. Furst, M.H. Butler, S. Xu, N. Grigorieff, and S.A. Goldstein. 2004. Ito channels are octomeric complexes with four subunits of each Kv4.2 and K^+ channel-interacting protein 2. *J. Biol. Chem.* 279:5549–5554.

Kin, Y., Y. Misumi, and Y. Ikehara. 2001. Biosynthesis and characterization of the brain-specific membrane protein DPPX, a dipeptidyl peptidase IV-related protein. *J. Biochem. (Tokyo).* 129:289–295.

Li, H.L., Y.J. Qu, Y.C. Lu, V.E. Bondarenko, S. Wang, I.M. Skerritt, and M.J. Morales. 2006. DPP10 is an inactivation modulatory protein of Kv4.3 and Kv1.4. *Am. J. Physiol. Cell Physiol.* 291: C966–C976.

Long, S.B., E.B. Campbell, and R. MacKinnon. 2005a. Crystal Structure of a Mammalian Voltage-Dependent Shaker Family K^+ Channel. *Science.* 309:897–902.

Long, S.B., E.B. Campbell, and R. MacKinnon. 2005b. Voltage Sensor of Kv1.2: Structural Basis of Electromechanical Coupling. *Science.* 309:903–908.

Nadal, M.S., A. Ozaita, Y. Amarillo, E.V. de Miera, Y. Ma, W. Mo, E.M. Goldberg, Y. Misumi, Y. Ikehara, T.A. Neubert, and B. Rudy. 2003. The CD26-related dipeptidyl aminopeptidase-like protein DPPX is a critical component of neuronal A-type K^+ channels. *Neuron.* 37:449–461.

O'Leary, M., and R. Horn. 1994. Internal Block of Human Heart sodium Channels by Symmetrical Tetra-alkylammoniums. *J. Gen. Physiol.* 104:507–522.

Perozo, E., R. MacKinnon, F. Bezanilla, and E. Stefani. 1993. Gating currents from a nonconducting mutant reveal open-closed conformations in Shaker K^+ channels. *Neuron.* 11:353–358.

Posson, D.J., P. Ge, C. Miller, F. Bezanilla, and P.R. Selvin. 2005. Small vertical movement of a K^+ channel voltage sensor measured with luminescence energy transfer. *Nature.* 436:848–851.

Ren, X., Y. Hayashi, N. Yoshimura, and K. Takimoto. 2005. Transmembrane interaction mediates complex formation between peptidase homologues and Kv4 channels. *Mol. Cell. Neurosci.* 29:320–332.

Roux, M.J., R. Olcese, L. Toro, F. Bezanilla, and E. Stefani. 1998. Fast inactivation in Shaker K^+ channels. Properties of ionic and gating currents. *J. Gen. Physiol.* 111:625–638.

Schoppa, N.E., and F.J. Sigworth. 1998. Activation of Shaker Potassium Channels. I. Characterization of Voltage-dependent Transitions. *J. Gen. Physiol.* 111:271–294.

Strop, P., A.J. Bankovich, K.C. Hansen, K.C. Garcia, and A.T. Brunger. 2004. Structure of a human A-type potassium channel interacting protein DPPX, a member of the dipeptidyl aminopeptidase family. *J. Mol. Biol.* 343:1055–1065.

Tombola, F., M.M. Pathak, and E.Y. Isacoff. 2006. How Does Voltage Open an Ion Channel? *Annu. Rev. Cell Dev. Biol.* 22:23–52.

Yifrach, O., and R. MacKinnon. 2002. Energetics of pore opening in a voltage-gated K^+ channel. *Cell.* 111:231–239.

Zagha, E., A. Ozaita, S.Y. Chang, M.S. Nadal, U. Lin, M.J. Saganich, T. McCormack, K.O. Akinsanya, S.Y. Qi, and B. Rudy. 2005. DPP10 modulates Kv4-mediated A-type potassium channels. *J. Biol. Chem.* 280:18853–18861.

Zagotta, W.N., T. Hoshi, and R.W. Aldrich. 1994. Shaker Potassium Channel Gating. III: Evaluation of Kinetic Models for Activation. *J. Gen. Physiol.* 103:321–362.

Zhou, W., Y. Qian, K. Kunjilwar, P.J. Pfaffinger, and S. Choe. 2004. Structural Insights into the Functional Interaction of KChIP1 with Shal-Type K^+ Channels. *Neuron.* 41:573–586.